Positron annihilation spectroscopy of solgel synthesized Ni(1-x)Mgx Onanoparticles

Anjan Das[1]
[1]*Department of Physics, A.P.C. Roy Government College, Siliguri, Darjeeling 734010, West Bengal, India*

Abstract- Nickel oxide (Ni1-xMnxO) nanoparticles doped with magnesium were synthesized withx = 0 to 0.05 by sol-gel method involving chemical reactions between the solutions of nickel nitrate hexahydrate and magnesium acetate. The nanocrystallites obtained after annealing of the precipitates for different durations were characterized by X- ray diffraction and high resolution transmission electron microscopy. The average sizes of the crystallites were obtained in the range 15 nm to 33.6 nm for the different samples. The synthesized samples showed high degree of purity and did not show any secondary phase up to 5% (x = 0.05) of Mg-doping. Excitonic bound states in NiO on Mg-doping was indicated by UV-Vis absorption studies. Positron lifetime and Doppler broadening spectroscopic studies were carried out on those samples to characterize the vacancy type defects and defect clusters/complexes. There were also indications to suggest positron annihilation at the crystallite surfaces owing to their sizes of nanometer order. Positron lifetimes decreased upon increase of Mg-doping. The coincidence Doppler broadened ratio curves and the variation of the lineshape parameter S also indicated clearly the effects of Mg-doping.
Keywords : Defects, doping, nanocrystallites, nickel oxide, optical absorption, positron annihilation, vacancies.

I. INTRODUCTION

Oxide nanoparticles have been drawing much attention in recent years because of their peculiar optical and electrical properties. [1-2]Properties of nanoparticles (electrical, optical, chemical, mechanical and magnetic) can be selectively controlled by engineering the size, morphology and composition due to their larger surface to volume ratio. Metal ion doping has been widely performed on semiconductors to minimize electron/hole recombination and enhance their absorption towards visible light region. [3-6]NiO has been considered as a promising material for a variety of applications such as solar cells, p-type transparent conducting electrodes, gas sensors and anode of lithium ion batteries to increase their energy density.

Experiments on transition metal (TM) ion-doped NiO samples have been done mainly for their dielectric and magnetic properties. [7-8]Themain focus mostly has been on the variation in the magnetic properties.The optical band gap, structural defects and defects-related properties especially at nanoscale dimensions still need in-depth investigation and the present work is a right step in this direction.Positron annihilation studies are very promising for this purpose by virtue of the high propensity of positrons to defects in solids and the ability to provide information as measurable changes in their annihilation characteristics. [9-10]

II EXPERIMENTAL DETAILS

2.1. Synthesis

There is no definite synthesis modelto produce transition ion-doped metal oxide nanoparticles of desired sizes and morphologies. Many researchers have reported various methods.Setoudeh et al[8]and Toboonsung et al [11]prepared nickel- magnesium and Fe doped NiO by mechanochemical and co - precipitation method. Barman et al [12]produced nanoparticles by self-assembling through thermal processes.In our work,manganese-doped nickel oxide nanoparticles were synthesized by the easy, economical and widely used sol-gel method. For the purpose of synthesis, we have used nickel nitrate hexahydrate(Ni(NO3)2.6H2O) andmagnesium acetate (Mg(CH3COO)2.4H2O) as starting materials. Two solutions have been prepared separatelyby dissolving 50 gm of Ni(NO3)2.6H2O and required amount of Mg(CH3COO)2.4H2O for the desired atomic percentage (at.%) of doping. The solvent was ethyl alcohol with double-distilled water in the ratio 1:2. The pH of the solutions were maintained in the acidic range by adding nitric acid and acetic acid to the Ni(NO3)2.6H2O and Mg(CH3COO)2.4H2O solutions respectively. The individual solutions were stirred for 1hour. These solutions were then mixed and stirred for 1 hourwith a magnetic stirrer. By this process six solutions have been prepared with different amounts of Mg(CH3COO)2.4H2O to obtain different percentages of doping. The atomic percentage value varies from 0 to 5.The solutions were kept for gelation for 2 days. Then the gels were evaporated to dryness at 70^{o} Cto get a green colored powder. Thereafter, all the powders were annealed at 400^{o} Cfor 3 hours and all the samples became light black in color after the annealing.

2.2. Structural characterization and optical absorption measurements

To determine the particle size and strain of each sample, x-ray diffraction measurements of the samples were carried out with a Bruker D8 advance diffractometer using incident Cu Ka (l = 1.5406 Å) radiation at 40 kV and 40 mA. All of the samples were scanned from 2Θ = 20o to 80owith a scanning speed of 2o per minute. The morphology and crystallite size of samples were studied by high-resolution transmission electron microscopy (HRTEM). The microscope used (FEI Model Technai S-twin) had a resolution 0.24 nm.

2.3. Positron annihilation measurements

Positron annihilation techniques are then applied to study the powdered synthesized samples. Positron lifetime and Doppler broadening measurements were carried out using a 10 μCi strong 22Na source. It was deposited in solution form and dried on a very thin (~ 2 mg cm-2) and well-annealed Ni foil whose extended portion is then folded to cover the source deposition. The source in this form is then kept immersed in the column of the powdered sample taken in a glass tube. The glass tube was continuously evacuated to avoid air and/or absorbed gases in between the crystallites and the powder settled down under its own weight. Thus the source and sample had been always kept in moisture-free conditions.

The positron lifetime spectrometer used for the measurements comprised of BaF2 scintillators coupled to XP2020Q photomultiplier tubes and the associated nuclear electronics constituting a standard slow-fast gamma-gamma coincidence set up. [13] The time resolution of the spectrometer obtained with the gamma rays of 60Co under the actual experimental settings to accept the 1.276 MeV and 0.511 MeV photopeaksof 22Na was 170 ps (full width at half maximum). For Doppler broadening measurements, two high pure germanium (HPGe) detectors of energy resolution 1.33 keVand 1.27keV at 0.511 MeV were used. About 3×106 and 1.5×106 counts were collected under each positron lifetime and Doppler broadened gamma ray spectrum respectively. In CDBS measurements, about 3×107 coincidence events were obtained under the two-parameter spectrum.

III RESULTS AND DISCUSSION

3.1. X-ray diffraction and TEM studies

Figure 1 shows the XRD patterns of Ni1-xMgxO samples with x = 0.0, 0.01, 0.03 and 0.05.The spectra ensured the purity of the phases as they revealed only the cubic phase of pure NiO and not any other phase. The main peaks were observed around 2θ values of 37.1°, 43.2°, 63.4°, 75.1° and 79.0°. The observed diffraction peaks are in good agreement with the standard values (JCPDS no. 24-0712). All the samples exhibited the main peaks corresponding to (111), (200), (220), (311) and (222) planes of face centred cubic structure. High doping (x = 0.05) did not alter the structure from NiO.Line broadening of the diffraction peaks indicate that the synthesized materials are composed of particles in the nanometer size range. It is clearly observed from the XRD patterns thatthe diffraction peaks become broader and less intense with the increase in doping concentration. It suggests that the particles become more and more nanocrystalline in nature and size with increasing concentration of doping.

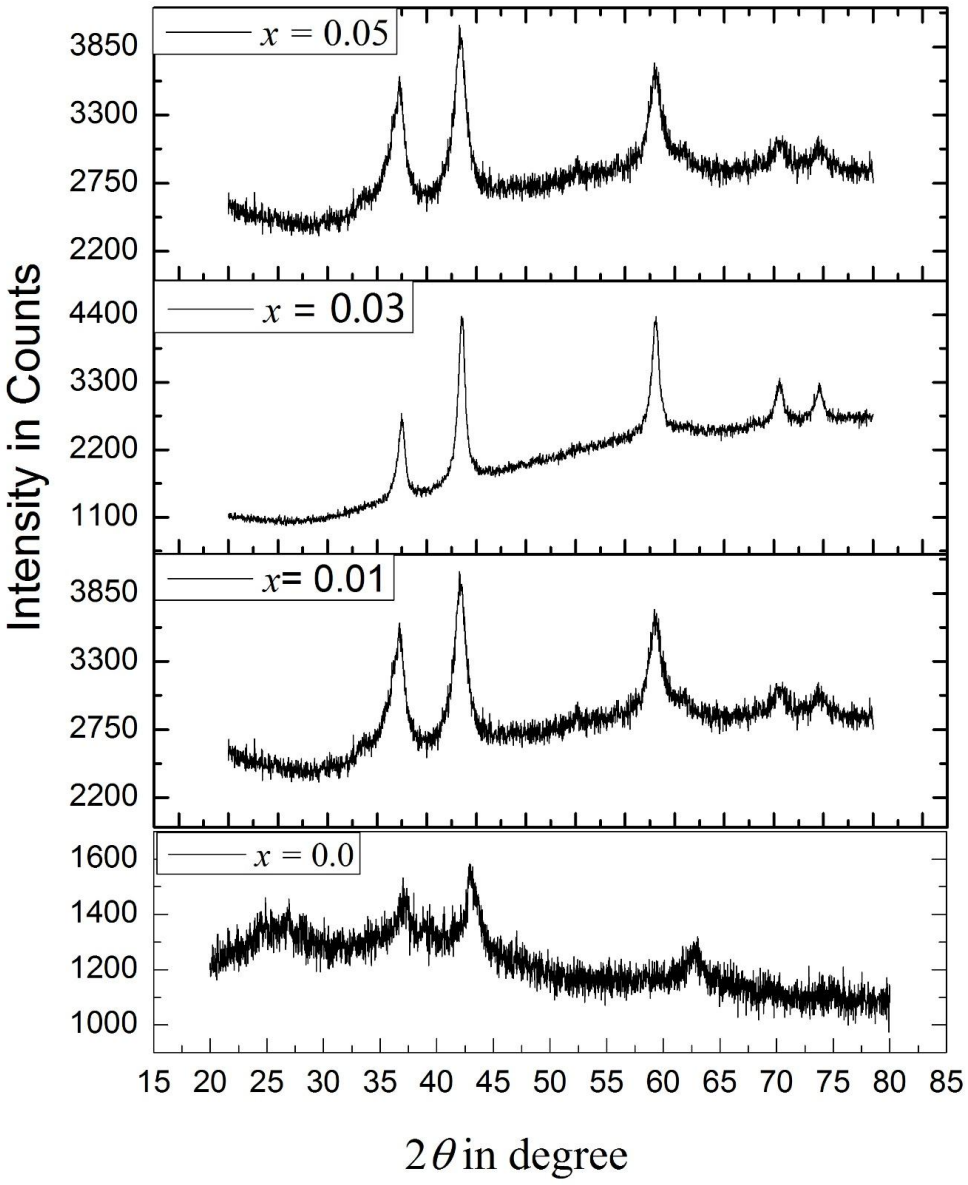

Figure 1.The XRD patterns of Ni1-xMgxO samples.

From the X-ray diffraction peak widths, the average crystallite sizes of the different samples were estimated by using the Debye-Scherrer equation[14]

$D = 0.9\lambda/(\beta\cos\theta)$ (1)

whereD is the average crystallite diameter, λ is the wavelength (CuK□ □ □used by the diffractometer, β is the line width at half–maximum and 2θ is the Bragg angle. We used the most intense peak (200) in the XRD patterns to calculate the average crystallite sizeand they varied from 15 nm to 33.6 nm. The crystallite sizes are plotted against the Mg doping concentration and are shown in Table 1. The crystallite sizes of the undoped sample are in a very narrow distribution range centred around 19 nm.The HRTEM figures 2(a) – 2(d) further verified this. It can be seen that each sample consists of hexagonal crystals of almost same size. The nanoparticles size calculated in the

HRTEM images approximately resembles with the particle size calculated from the XRD analysis. For example, the calculated average size for undoped (Figure 2 (a)) and the 3 at.% Mg-doped (Figure 2 (b)) samples are 19nm and 33 nm respectively.

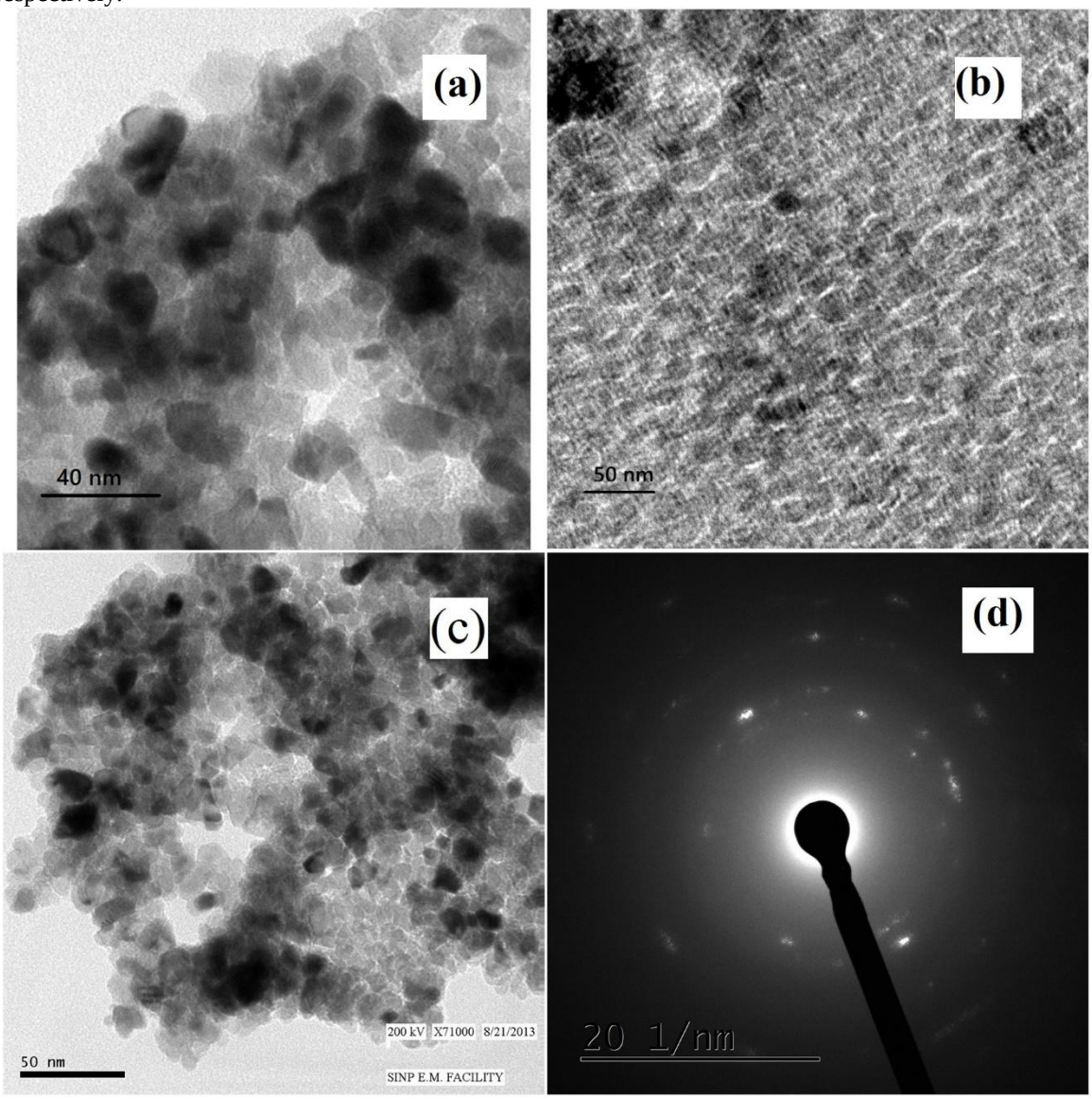

Figure 2. TEM and HRTEM images of the differently doped samples. (a) x = 0, (b) x = 0.03, (c) x = 0.04, (d) x = 0.05, indicating the hexagonal crystals of almost same sizes in each.

Besides this, lattice fringes can also be observed for the different lattice planes. It is observed fromTable 1that there is an initial increase of the crystallite size till 0.03 at.% of doping and beyond this concentration, the sizes of the crystallites gradually got reduced. The initial increase of the crystallite size seemed to result from the cancellation ("recombination") of a number of existing cationic vacancies (VNi2-) by the doped Mg2+ ions and the corresponding push imparted to the neighbouring ions. Crystallite size decreased thereafter with further doping. The ionic radius of Mg2+ (0.72Å)[15] is larger than that of Ni2+ (0.69Å)[15] and which may cause additional strain in the lattice with increased doping. It is likely that a large number of Mg2+ ions are therefore be accommodated on the crystallite surfaces and.It caused larger surface to volume ratio to cope with the increased percentage of doping, in other words, smaller crystallites. Upon large percentage of doping, the phase purity was not retained. It could be seen that the NaCl structure of pure NiO remains the same uptox = 0.05 and the nickel-magnesiumoxide (NiMgO) has the same space group Fm3m as that of NiO. Beyond this concentration, the phase stability is lost and further effects or changes have not been considered in this work.

Concentration (at. %)	nanocrystallite size (nm)	Lattice constant(a) (Å)	Change in lattice constant (Å)	Band gap (eV)
0	18.3	4.234 $\pm$ 0.002	0.039	4.5
1	15.0	4.231 $\pm$ 0.002	0.036	4.65
2	25.2	4.230 $\pm$ 0.002	0.035	4.78
3	33.6	4.228 $\pm$ 0.002	0.033	4.85
4	27.0	4.231 $\pm$ 0.002	0.036	4.98
5	21.2	4.233 $\pm$ 0.002	0.038	5.19

Table-1. Doping concentration, crystallite sizes, lattice constants, change in lattice constants and band gap of the annealed samples.

We further observe from Figure 1 that the peaks have gradually shifted towards higher 2θ values on increasing the doping concentration (uptox = 0.03) which implies the contraction of the lattice. Bulk NiO has a lattice constant 4.195 Å. The lattice constants (a) of the different samples were estimated from the X-ray diffraction data by combining the Bragg's equation with the interplanar spacing (d) and getting the relation

$$\frac{4Sin^2\theta}{\lambda^2} = \frac{1}{d^2} = \frac{h^2 + k^2 + l^2}{a^2} \quad (2)$$

Table 1 shows the variation of the lattice constant with the concentration of Mg-doping of NiO. The lattice constants of all the samples are found slightly increased from its bulk value.The lattice is contracting with increasing concentration of doping uptox = 0.03. This fact can be attributed to the occupancy of Ni2+ ionic monovacancies (VNi2-) by Mg2+ ions.Manuel Diehm et al [16] have made a detailed analysis of the effect of sizes of nanoparticles of oxides on the lattice parameter changes and, according to them, strain mediated by structural defects like vacancies is a major cause of lattice expansion in metal oxide nanoparticles and hence, the reverse observation of contraction can be seen as a result ofat least a fraction of the existing vacancies being annulled by their occupancy by self- or closely-related species of cations. With the addition of more Mg2+ ions (i.e., beyond x = 0.03), the actual process of substitution dominates where a large number of Ni2+ ions from their respective lattice sites are being removed and their positions then occupied by the doped Mg2+ ions. As mentioned earlier, the ionic radius of the latter is higher than that of Ni2+(0.69 Å) [15] and hence the substitution process will result into additional strain and the lattice expands to contain it, without leading to the necessity of undergoing any structural transformation, at least upto the highest concentration of doping, x = 0.05, used in this work.
A view of the changes in lattice constants □ a versus the crystallite sizesis given in Table 1. As discussed above, it also suggests a two-fold evolution of the material structure itself with increasing Mg2+ concentration. However, for vacancy concentration alone to be a cause for lattice expansion, the log-log plot of the change in lattice parameter versus the crystallite size (D) needs to be 1/D dependent [16] whereas it is not in the present case. It is possible that nature and ionic radii of the doped ions may also have affected the lattice parameter changes, as explained above.

3.2. Optical absorption studies

The optical absorption spectra in the range from 200 to 600nm for the nanocrystalline samples are presented in Figure 3. The figure shows that the absorption edge wavelength (~ 325 nm [17]) of bulk NiO is fairly blue-shifted and excitonic absorption peaks of the as-prepared undoped and magnesium-doped samples appear around 240 nm.The optical band gap Egof the individual samples was calculated from the spectra using Tauc's relation αhν = A(hν-Eg)n where A is a constant, hν is the photon energy and n depends on the nature of transition. n is equal to 1/2 and 2 for direct and indirect transitions respectively. It is well known that NiMgO nanoparticles are direct band gap semiconductors.[17]Hence the optical band gap for the annealed samples can be obtained by extrapolating the linear portion of the (αhν)2vs. hν curve to zero. It is obvious that the band gap increases from a value of 4.5 eV for x = 0.0 to 5.19 eV for x = 0.05.Significantly, all these values are higher than theband gap energy Eg = 3.75 eV for bulk NiO.

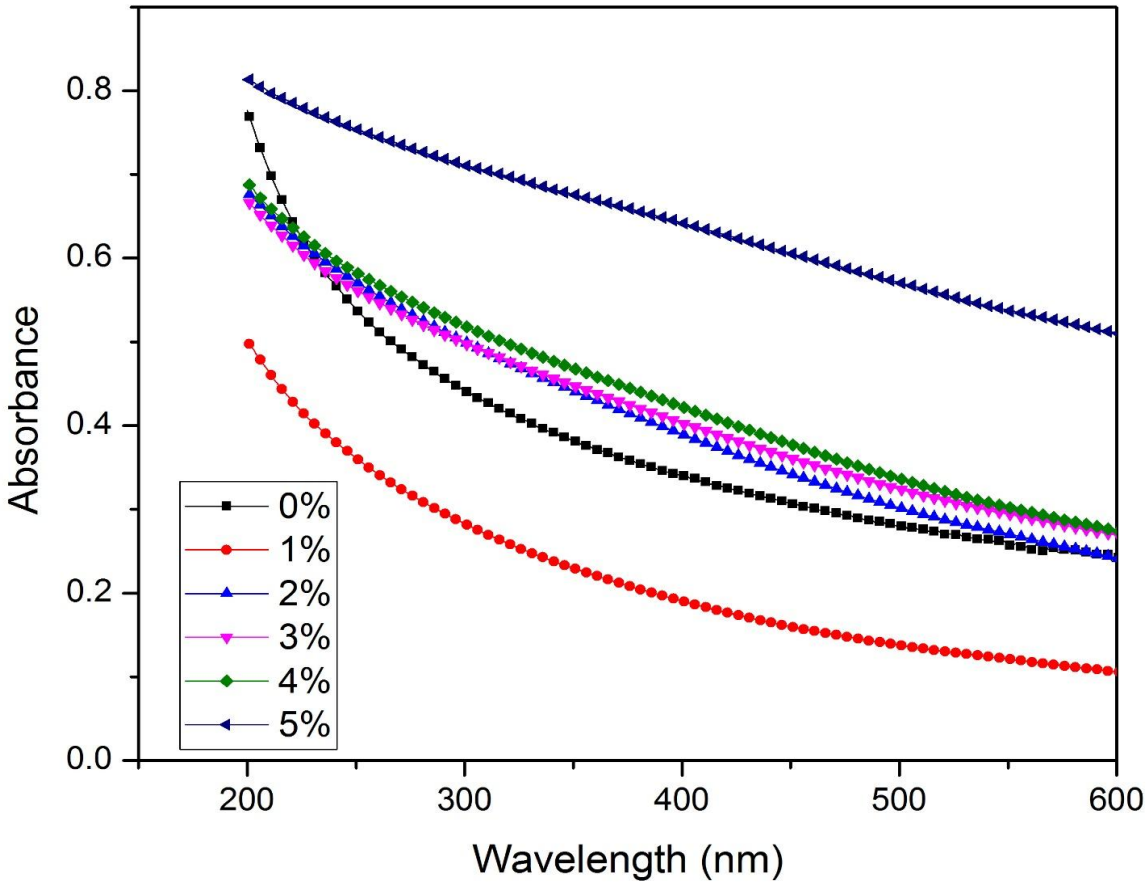

Figure 3. The optical absorption spectra of the nanocrystalline Mg-doped NiO samples.

The optical absorption behavior are explained by Kinoshita et al [18]. According to them the absorption of low energy photons that is uptox = 0.03 are attributable to the 2p-3d charge transfer transitions within NiO. But they have assigned the high energy, i.e. > 4.8 eV, photon absorptions to 2p-4s transitions within NiO and MgO when Mg2+ concentration increases.

3.3. Positron annihilation studies

The positron lifetime spectra are peak-normalized and plotted in Figure 4. The long-decaying nature of the spectra indicates the presence of extended positron lifetimes and the non-overlapping curves reflect definite variations in the lifetimes and intensities involved. The spectra was analysed with the program PALSfit22. The source contribution has been deleted, instrumental resolution has been deconvoluted and background has been subtracted. An average linear background is estimated from a region far away from the decaying tails of the spectra and is subtracted from each channel. The lifetimes and intensities due to positrons annihilating from materials other than the sample are normally obtained from a trial spectrum of a well-annealed sample (single crystalline Si procured from Johnson Matthey, USA in this case) of high purity (99.999%) and analyzing it for its known single lifetime (~ 220 ps for Si). The source had been prepared on a previously annealed Ni foil of very low thickness (~2 mgcm-2) which is folded along a line outside the periphery of the source deposited area to cover it and then used for experiments. The intensity of the positron lifetime in Ni foil is sample-dependent and is separately calculated using the equation given by Bertolaccini et al. [23]The other intensities are obtained from the spectrum of Si, which also gave the instrumental resolution function to analyze the experimental spectra.

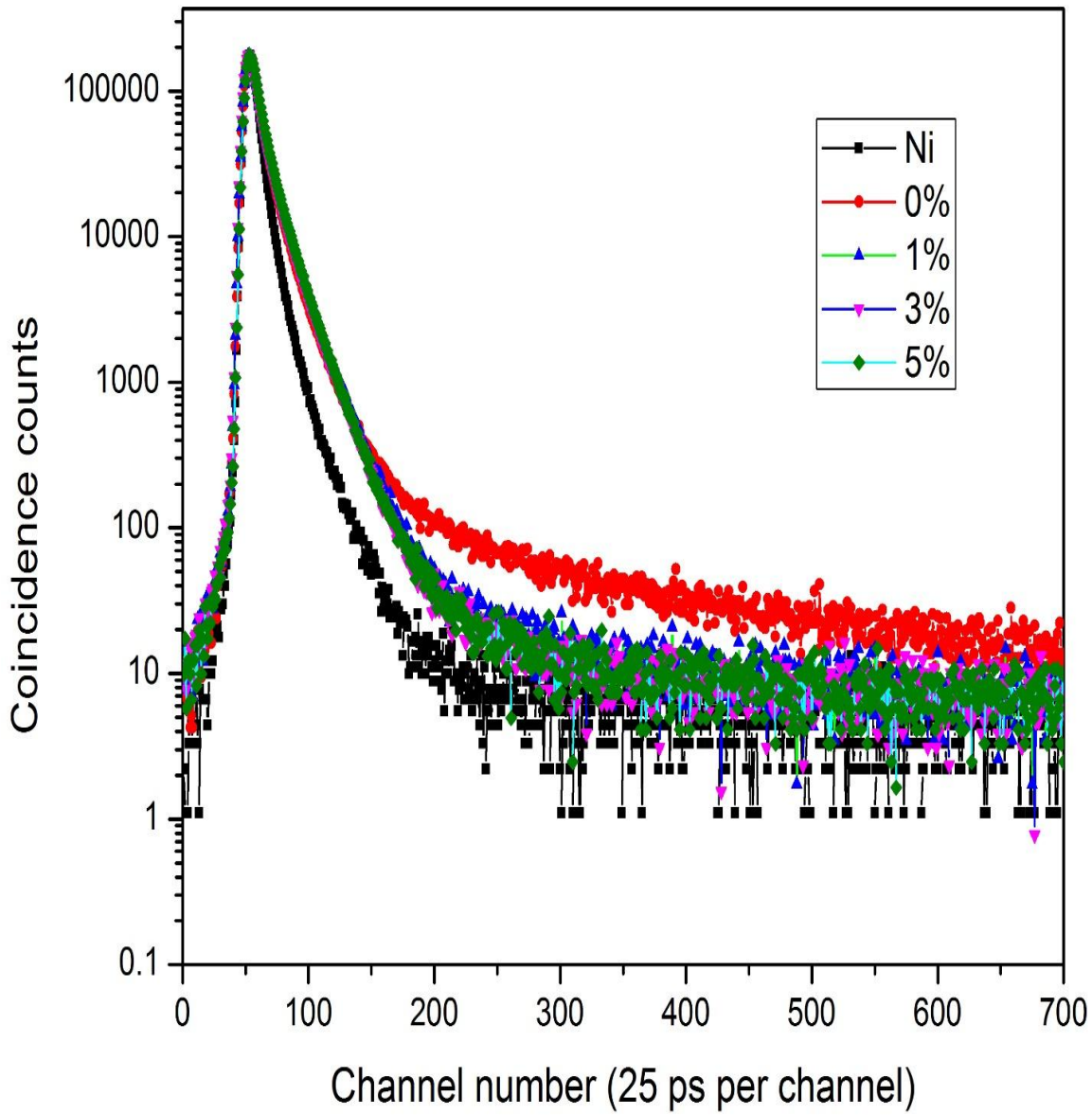

Figure 4. Peak-normalized positron lifetime spectra of some of the samples.

The resolved positron lifetimes and their intensities due to the sample can be understood from Figures 5 and 6 where their variations against the concentration of doped Mg2+ ions are illustrated. From each spectrum one can get three lifetimes denoted as □1, □ 2 and □ 3 in their ascending order of magnitudes and with respective relative intensities I1, I2 and I3. In the undoped NiO sample, we obtained □ 1 = 190ps, □ 2 = 446ps and □ 3= 2560ps. The longest lifetime, which is of the order of nanoseconds, comes from orthopositronium (o-Ps) formation and subsequent annihilation at the intercrystallite regions. o-Ps atoms are bound states of one electron and one positron each and have very long lifetime (~ 142 ns) in vacuum but can be reduced to only a few nanoseconds due to 'pick-off' process in materials. [9]

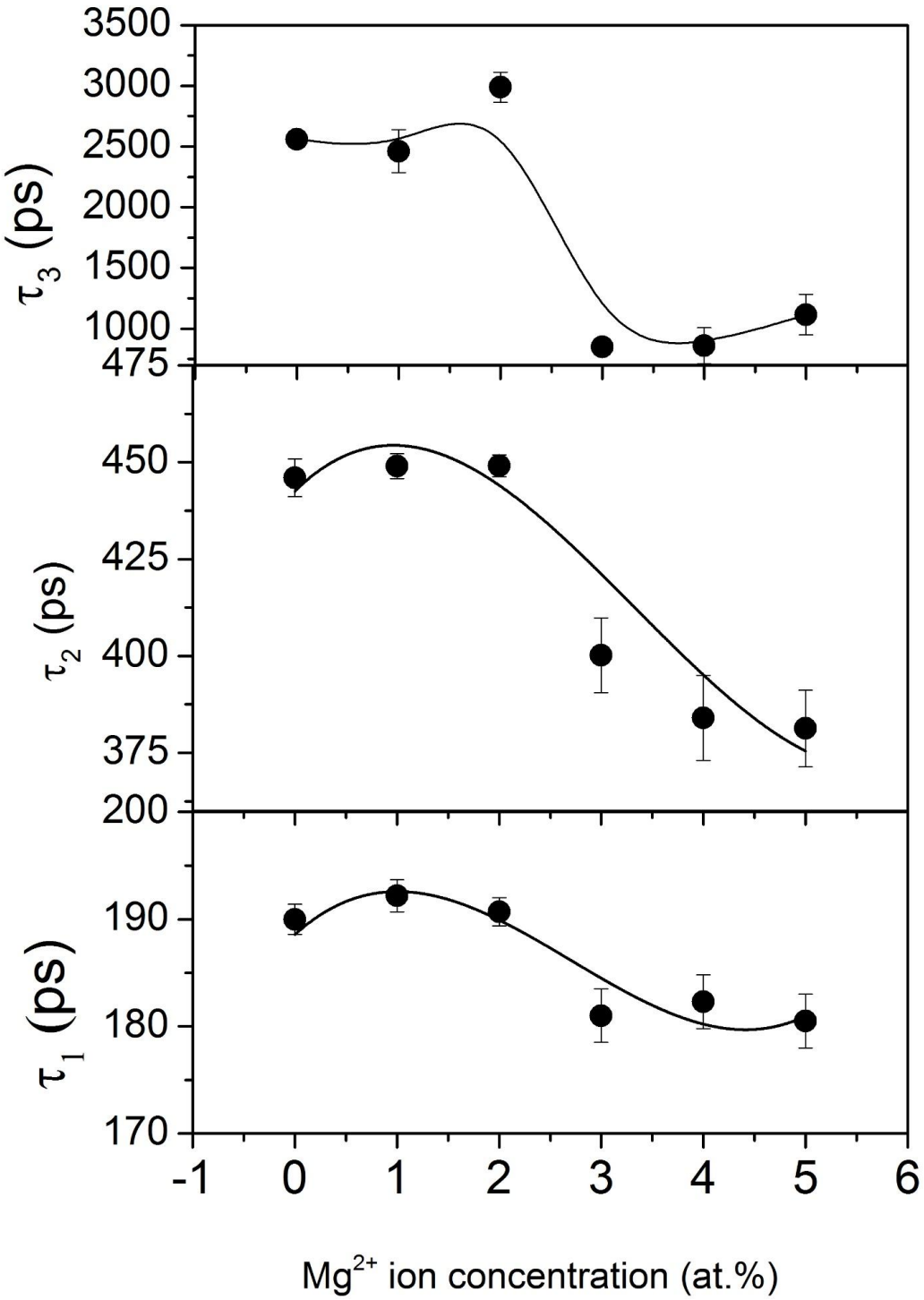

Figure 5. The resolved positron lifetimes in the different samples plotted versus the Mg-doping concentration.

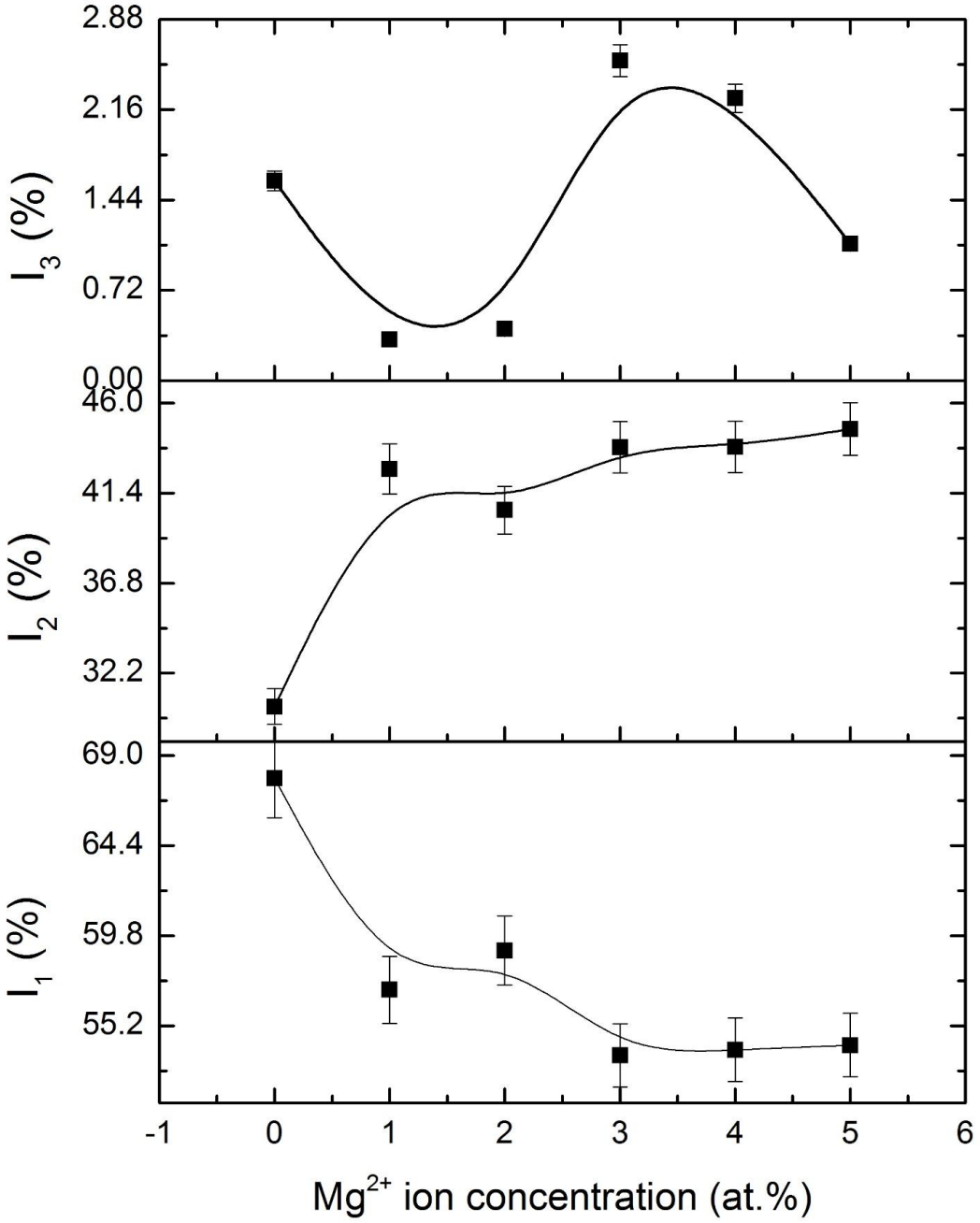

Figure 6. The intensities of lifetimes in different samples.

The intensity of this component normally is used to be small (~ 1-4%) but still makesits presence strongly felt in porous condensed material media. The intermediate defect-specific lifetime 2 is often admixed by crystallite surface-related positron lifetimes in nanocrystalline solids. To get more insight into this, a"bulk" positron lifetime was calculated (b)forNiOusing the equation

$$\frac{1}{\tau_b} = \frac{I_1}{\tau_1} + \frac{I_2}{\tau_2} + \frac{I_3}{\tau_3} \quad (3)$$

and obtained it as 228 ps. The reported positron lifetime b= 110 ps in bulk NiO[24] is considerably less than this value. The nanocrystallinity of the samples is also a reason since the positrons which are not trapped in any of the defects within the crystallites are likely to thermally diffuse over to the surfaces and get annihilated from there. In bulk crystalline solids, the thermal diffusion lengths of positrons are around 50-100 nm.[25] In nanocrystalline

particles and films, this has been reduced to 10 – 35 nm[26,27] and therefore the nanoparticles of sizes in the range 15 – 33.6 nm in this work are likely spread across this limit. It can be safely said that even the smallest lifetime component is having a contribution in it from vacancy-type defects on the surface of the nanocrystallites.

The presence of vacancy cluster-type defects within the interior of the nanocrystallites can be predicted from the second positron lifetime □ 2 = 446 ps in the undoped sample. The lifetime for clusters composed of a few monovacancies are shorter. In bulk solids, positron lifetime normally gets saturated in vacancy clusters composed of more than 10-15 monovacancies. As □ 2 in the present work is still found varying with the changes in doping concentration and the crystallitesize is still below the limit of saturation the defects must be smaller vacancy clusters. However, considering the large values of this component, it is still likely that □ 2 is an admixture of two lifetimes, one that is relatively less to the other and sensitive to the changes in Mg^{2+} ion concentration and crystallite sizes and the other one rather insensitive and almost saturated. There could be clusters of vacancy-type defects within the nanocrystallitescomposed of neighbouring Ni^{2+} (say, m in number) and O^{2-} vacancies (n) such that $m \geq n$. For the case $m<n$, the overall charge of the cluster of configuration mVNinVO will be positive and positron trapping is a near impossibility due to the repulsion. Positrons are attracted by vacancy clusters which are neutral or strongly negatively charged. The larger and the near-saturated positron lifetime admixed in □ 2 originates from positron trapping in microvoid-type defects at the intersection of the interfaces of two or more nanocrystallites and has been a common feature of several nanomaterials in which the crystallites are either not well separated or get agglomerated.

The variation of the positron lifetimes and their intensities depicted in the figures 5 and 6indicates the effects of Mg doping on the nanocrystalline structure and composition. Their variation can be classified into two regions. In the range of doping x = 0 to 0.02, all the positron lifetimes are higher than other highly doped samples whereas the defects-component intensity I2 has a substantial rise. The latter observation seems to apparently contradict the earlier interpretation given in terms of the cancellation of a number of Ni^{2+} monovacancies by Mg^{2+} ions. Moreover, the sizes of the nanocrystallites have also drastically decreased from about 18 nm (for x = 0) to ~ 15 nm (x = 0.01) that should rule out enhancement in surface annihilation probabilities at this stage. However, this particular instance of agglomeration of nanocrystallites can result into more number of microvoid-type defects at the intersection of the interfaces and I2 consequently can show a substantial increase (Figure 6). At the same time, the positron lifetime □ 2 decreases to indicate that the sizes of the vacancy clusters mVNinVO decreases as a certain number (<m) of Ni^{2+}monovacancies (VNi) are recombined with Mg^{2+} ions.

Inporous and amorphous materials [28, 29]the lifetime □ 3 of orthopositronium atoms directly is sensitive to the size of the free volume cavities, and even in nanocrystalline materials, it can vary according to the structure and environment of the intercrystalline regions. □ 3 is steadily increasing with increasing concentration of Mg-doping and it can be understood as a direct effect of increasein crystallite sizes. As the nanocrystallites become smaller in size, the width of the intercrystallite region can be significantly reduced and the material can be better compacted. This effect is observed beyond x = 0.02. At the same time, X-ray diffraction patterns are conspicuous to rule out any indication of unincorporated traces of Mg^{2+} ions and hence the observed decrease of □ 3 is purely an effect of the increased proximity of the nanocrystallites. When □ 3 is decreasing, the corresponding intensity I3 is increasing (for x> 0.02) as shown in Figure 6 and this can be understood as an effect of more number of positrons diffusing out of the crystallites when the crystallites are reducing in their sizes (Table 1).

The almost no change of trend in lifetimes and their intensities other than I3 for the sample with x = 0.05 can be attributed to Mg^{2+} ion segregation outside the grain boundaries which will be evident from coincidence Doppler broadening experiments. [30]The CDBS measurements is carried out with a view to understand the change in elemental surroundings of the positron trapping defects and the information is sought to be derived from the ratio curves shown in Figure 7. The individual one-dimensional projection of the events are divided by identical projection of a well-annealed Ni sample within E1+E2 = 1022±2.4 keV on the E1-E2 axis. The curves thereby represent the electron

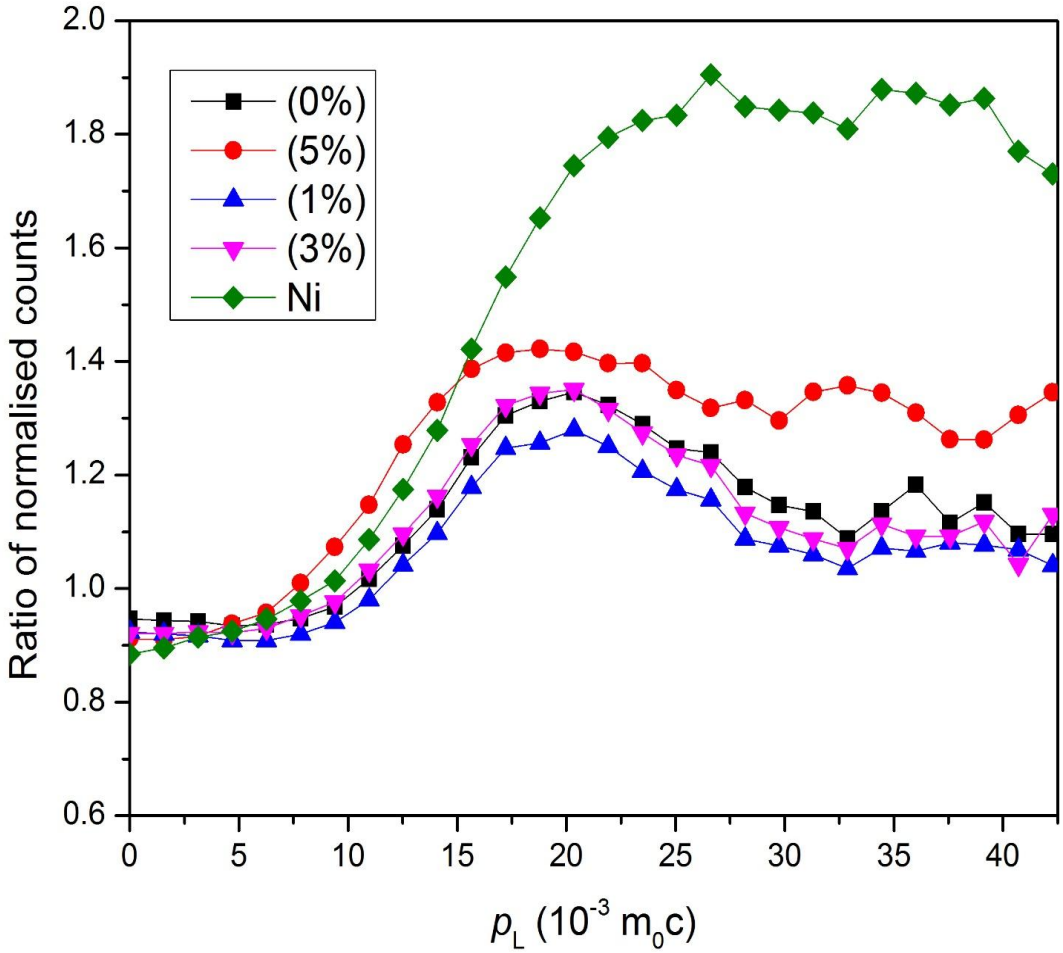

Figure 7. The ratio curves generated from the CDB spectra of the different samples with respect to the corresponding spectrum of a well-annealed Ni sample.

momentum distribution of the core electrons from oxygen ions surrounding the positron trapping defects. The absence of a prominent peak, normally observed in the case of annihilation with the 2p electrons of oxygen [26, 29], could be due to the presence of a surface oxide layer on the Ni sample used. Two features are, however, remarkable in this figure. The curves corresponding to the undoped (x = 0) and the samples doped with relatively low concentration (x = 0.01 and 0.02) of Mg2+ ions almost fully overlap over a wide range of electron momentum indicating that the annihilations are taking from positron trapping defects dominated by cationic vacancies. Secondly, the curve of the x = 0.05 sample has deviated to the lower momentum side. As τ3 and I3 has also significantly decreased it appears to point about the likely segregation of Mg2+ ions on grain boundaries of highest doped sample in minute amount. It is worth to mention in this context here that an identical observation in Mn-doped ZnOnanocrystals has been earlier reported. [30]

The Doppler broadened positron annihilation lineshape parameter Sis depicted in Figure 8. The S parameter had been derived here as the ratio of the counts over 511±0.64 keV to the total counts under the spectrum spreading over 511±8 keV. By definition, this parameter is the relative percentage of low momentum electron annihilation events

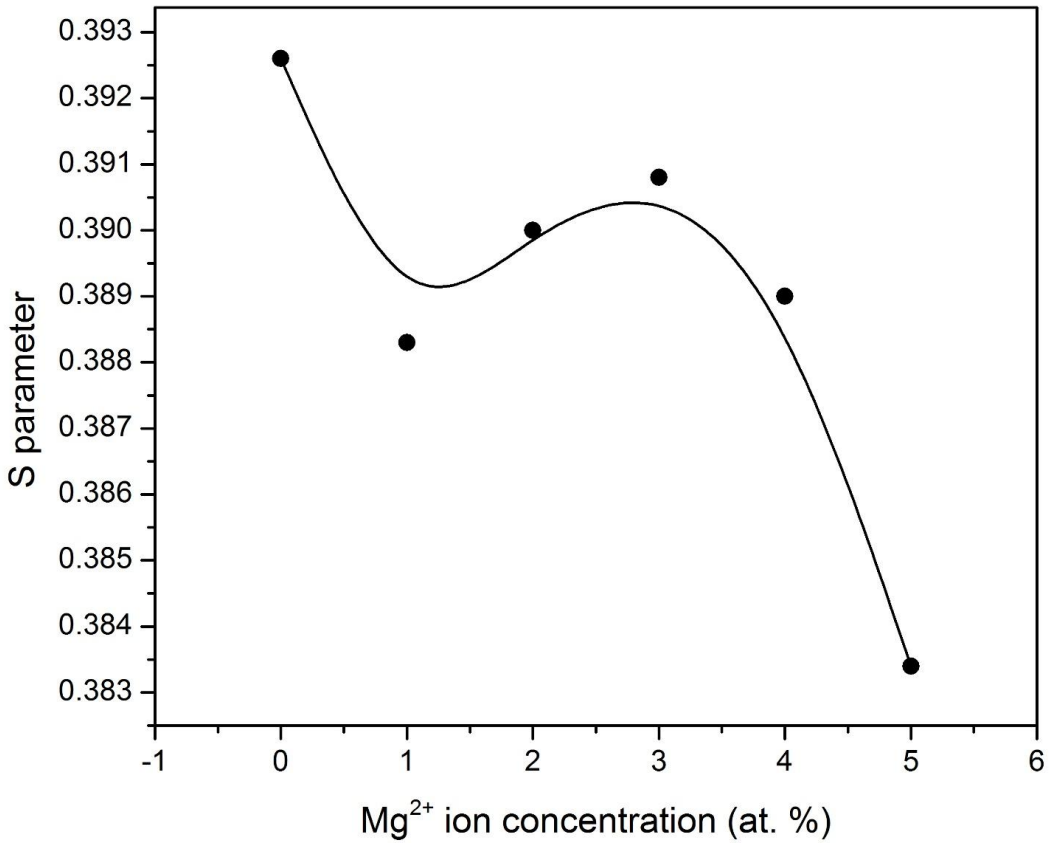

Figure 8. The variation of the Doppler broadened positron annihilation lineshape parameter S versus the Mg-doping concentration in the different samples.

and is proportional indirectly to the total defect volume within the material. S exhibits remarkable changes as the doping percentage is increased. It can be seen that the S parameter has altered its trend two times upon increase of doping percentage. The undoped sample has the highest value of S parameter and it suffers a huge decrease on Mg-doping. It is observed from Figure 7 that the peaks of the spectra of the undoped and doped samples (x = 0.1 and 0.3) stays at the same place. This suggests that positrons are annihilating with the electrons of Ni2+ as well as Mg2+ in those doped samples in the same manner. It can also be observed that the positron lifetime τ2is decreasing by its value and indicates the reduction of size of positron trapping site. In other words, a Ni2+monovacancy(VNi2-) is now occupied by aMg2+ ion. Since S denotes the fraction of low momentum electrons, it increases therefore as a result of increased annihilation with the Mg2+ electrons. The peak shifting to the high momentum side inCDBS ratio curve of the x = 0.05 (i.e.,5 at.%) sample andthe decrease ofS parameter indicatessegregation of Mg2+.

IV. SUMMARY AND CONCLUSIONS

The results of positron annihilation studies of the defects and their modifications under Mg-doping in NiOwhich is a wide band gap semiconductor with great potential for future technological applications has been presented in this paper. The sol – gel process of synthesis, characterization and properties of this material, in view of technical application, appeared to be interesting in their own merit. The synthesis procedure of this work for preparing both the undoped and Mg-doped NiO is very fruitful as,for each sample, the nanocrystallitesizes were efficiently controlled. The results obtained for crystallite size from XRD and HRTEM images confirm the nanocrystalline nature of the synthesized products.The defect structures in chemically synthesized Ni1-xMgxO are studied using positron lifetime spectroscopy that indicated the association of the doped Mg2+ ions with the existing vacancy clusters through a decrease of positron lifetime components and shift in the CDBS peaks during x = 0 to 0.02.Highdoping i.e. after x = 0.02 certainly indicated the modification of the defectsorroundings by the doped ions and also the Mg2+ ions segregation was indicated by positron lifetimes and CDBS spectra. At the initial doping concentrations, the crystallite sizes momentarily increased due to vacancy type defects being recombined with some of the doped ions. However, substitution-induced strain soon caused the sizes to start reducing again. There was conspicuous changes in the lattice parameter too which could again be attributed to the strain effects. UV-Vis

spectroscopy clearly indicated the formation of excitonic bound states on increased percentage of doping that has been rarely found by other experiments.

V. ACKNOWLEDGEMENTS

The author thanks the staff of the HRTEM facility of Saha Institute of Nuclear Physics, Kolkata for their help and cooperation in taking the images of the undoped sample. Thanks are also due to Dr. Goutam Das of National Metallurgical Laboratory, Jamshedpur for HRTEM figures of the doped samples and the X-ray diffraction measurements.

VI. REFERENCES

[1] Peidong Yang, The Chemistry of Nanostructured Materials, World Scientific, Singapore2003.
[2] P. Moravec, J. Smolík, H. Keskinen, J. M. Mäkelä, S.Bakardjieva and V. V. Levdansky, "NiOx Nanoparticle Synthesis by Chemical Vapor Deposition from Nickel Acetylacetonate",Mater. Sci. Appl., 2, pp - 258-264, 2011.
[3] A. Zaleska, Recent Patents on Engineering, 2, pp- 157-164, (2008).
[4] S. Kant and A. Kumar,"A comparative analysis of structural, optical and photocatalytic properties of ZnO and Ni doped ZnOnanospheres prepared by sol-gel method" Adv. Mat. Lett.,3(4), pp - 350-354, 2012.
[5] A. Lipovsky, A. Gedanken and R. Lubart,"Visible light-induced antibacterial activity of metaloxide nanoparticles",Photomed. Laser Surg., 31(11), pp - 526-530, 2013.
[6] P. Pongwan, B. Inceesungvorn, K. Wetchakun, S. Phanichphant and N. Wetchakun,"Highly Efficient Visible-Light-Induced Photocatalytic Activity of Fe-doped TiO2 Nanoparticles",Engg. Journal, 16(3), pp - 143-151, 2012.
[7] P. Mallick and N. C. Mishra, "Evolution of Structure, Microstructure, Electrical and Magnetic Properties of Nickel Oxide (NiO) with Transition Metal ion Doping",American J. Mater. Sci. 2(3), pp - 66-71, 2012.
[8] N. Setoudeh, C. Jamani, and M. Sajjadnejad, "Mechanochemical Synthesis of Nanostructured MgXNi(1-X)O Compound by Mg-NiO Mixture",Jour. of Ultrafine Grained and Nano. Mat.50(1), pp - 51-59, 2017.
[9] R.W. Siegel, "Positron annihilation spectroscopy",Ann. Rev. Mater. Sci.,10, pp- 393-425, 1980.
[10] K. Iwata, "Positron annihilation on atoms and molecules",Ph. D. Thesis, University of California, San Diego, 1997.
[11] B. Toboonsung, "Structure, Magnetic Property and Energy Band Gap of Fe-Doped NiO Nanoparticles Prepared by Co-Precipitation Method", Key Engineering Materials, Vol. 751, pp. 379-383, 2017.
[12] M. Barman, S. Paul and A. Sarkar,"Electronic properties in Mn doped and pure NiO clusters", AIP Conf. Proc. 1536, pp - 427-428, 2013.
[13] P.M.G. Nambissan, in "Nanotechnology : Synthesis and Characterization (Volume 2)", Eds. Shishir Sinha, N.K. Navani, J.N. Govil, Studium Press LLC, Houston, pp - 455-491, (2013).
[14] B.D. Cullity, Elements of X-ray Diffraction, Addison-Wesley Publishing Company, Inc., Reading, Massachusetts ,(1956).
[15] Stankic, S, Sterrer, M, Hofmann, P, Bernardi, J, Diwald, O and Kno1zinger, E,"Novel Optical Surface Properties of Ca2+-Doped MgONanocrystals",Nano Letters 5(10), pp - 1889-1893, 2005.
[16] http://www.webelements.com/manganese/atom_sizes.html.
[17] P. M. Diehm, P. Ágoston and K. Albe,"Size-Dependent Lattice Expansion in Nanoparticles: Reality or Anomaly?"ChemPhysChem (Special Issue: Nanomaterials),13,pp -2443-2454, 2012.
[18] J. Wang, L. Wei, L. Zhang, C. Jiang, E. S. Kong and Y. Zhang, "Preparation of high aspect ratio nickel oxide nanowires and their gas sensing devices with fast response and high sensitivity"J. Mater. Chem.,22, pp - 8327-8335, 2012.
[19] K. Kinoshita ,T. Nishida ,S. Shingubara,M. Inada andT. Saitoh, "Optical absorption properties of Ni1−xMgxO thin films", IEEE International Meeting for Future of Electron Devices, Kansai,2017.
[20] J.V. Olsen, P. Kirkegaard, N.J. Pedersen, and M. Eldrup,"PALSfit: A new program for the evaluation of positron lifetime spectra." Phys. Stat. Sol. C. 4,pp - 4004-4006, 2007.
[21] M. Bertolaccini and L. Zappa,"Source-supporting foil effect on the shape of positron time annihilation spectra."Nuo. Cim. B. Seri.10. 52(2), pp - 487-494, 1967.
[22] B. Barbiellinii, P. Genoud and T Jarlborg,"Calculation of positron lifetimes in bulk materials." J. Phys.: Condens. Matter, 3, pp - 7631-7640, 1991.
[23] Y. Zhang, X. Ma, P. Chen, D. Li, X. Pi, D. Yang and P. G. Coleman,"Enhancement of electroluminescence from TiO2/p+-Si heterostructure-based devices through engineering of oxygen vacancies in TiO2." Appl. Phys. Lett. 95, pp - 252102-252103, 2009.
[24] T. Ghoshal, S. Biswas, S. Kar, S. Chaudhuri, and P. M. G. Nambissan,"Positron annihilation spectroscopic studies of solvothermally synthesized ZnOnanobipyramids and nanoparticles." J. Chem. Phys. 128, pp - 747021-747026, 2008.
[25] B. Bergersen ,"Positron diffusion in metals."Solid Stat. Commun. 15, pp - 1377-1380, 1974.
[26] M. Eldrup, D. Lightbody, and J.N. Sherwood, "The temperature dependence of positron lifetimes in solid pivalic acid."Chem. Phys. 63, pp - 51 – 58, 1981.
[27] H. Nakanishi, S. J. Wang, and Y. C. Jean, in "Positron Annihilation Studies of Fluids," edited by S. C. Sharma, World Scientific,Singapore, pp - 292-296, 1988.
[28] P. Asoka-Kumar, M. Alatalo, V. J. Ghosh, A. C. Kruseman, B. Nielsen and K. G. Lynn, "Increased elemental specificity of positron annihilation spectra."Phys. Rev. Lett. 77, pp - 2097-2100, 1996.
[29] T. Ghoshal, S. Kar, S. Biswas, S.K. De, and P.M.G. Nambissan, "Vacancy type defects and their evolution under Mn substitution in single crystalline ZnOnanocones studied by positron annihilation."J. Phys. Chem. C113, pp - 3419-3425, 2009.
[30] B. Roy, B. Karmakar, P. M. G. Nambissan, and M. Pal, "Mn Substitution effects and associated defects in ZnO nanoparticles studied by positron annihilation."Nano. 6(2), pp - 173-183, 2011.